



## UvA-DARE (Digital Academic Repository)

### Cytochrome $cbb_3$ of Thioalkalivibrio is a $\text{Na}^+$ -pumping cytochrome oxidase

Muntyan, M.S.; Cherepanov, D.A.; Malinen, A.M.; Bloch, D.A.; Sorokin, D.Y.; Severina, I.I.; Ivashina, T.V.; Lahti, R.; Muyzer, G.; Skulachev, V.P.

**DOI**

[10.1073/pnas.1417071112](https://doi.org/10.1073/pnas.1417071112)

**Publication date**

2015

**Document Version**

Author accepted manuscript

**Published in**

Proceedings of the National Academy of Sciences of the United States of America

[Link to publication](#)

**Citation for published version (APA):**

Muntyan, M. S., Cherepanov, D. A., Malinen, A. M., Bloch, D. A., Sorokin, D. Y., Severina, I. I., Ivashina, T. V., Lahti, R., Muyzer, G., & Skulachev, V. P. (2015). Cytochrome  $cbb_3$  of Thioalkalivibrio is a  $\text{Na}^+$ -pumping cytochrome oxidase. *Proceedings of the National Academy of Sciences of the United States of America*, 112(25), 7695-7700.  
<https://doi.org/10.1073/pnas.1417071112>

**General rights**

It is not permitted to download or to forward/distribute the text or part of it without the consent of the author(s) and/or copyright holder(s), other than for strictly personal, individual use, unless the work is under an open content license (like Creative Commons).

**Disclaimer/Complaints regulations**

If you believe that digital publication of certain material infringes any of your rights or (privacy) interests, please let the Library know, stating your reasons. In case of a legitimate complaint, the Library will make the material inaccessible and/or remove it from the website. Please Ask the Library: <https://uba.uva.nl/en/contact>, or a letter to: Library of the University of Amsterdam, Secretariat, P.O. Box 19185, 1000 GD Amsterdam, The Netherlands. You will be contacted as soon as possible.

# Cytochrome *cbb*<sub>3</sub> of *Thioalkalivibrio* is a Na<sup>+</sup>-pumping cytochrome oxidase

Maria S. Muntyan<sup>a,1</sup>, Dmitry A. Cherepanov<sup>a</sup>, Anssi M. Malinen<sup>b</sup>, Dmitry A. Bloch<sup>a,c,2</sup>, Dmitry Y. Sorokin<sup>d,e</sup>, Inna I. Severina<sup>a,3</sup>, Tatiana V. Ivashina<sup>f</sup>, Reijo Lahti<sup>b</sup>, Gerard Muyzer<sup>g</sup>, and Vladimir P. Skulachev<sup>a,1</sup>

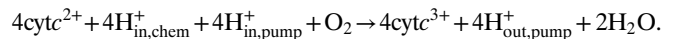
<sup>a</sup>Belozersky Institute of Physico-Chemical Biology, Lomonosov Moscow State University, Moscow 119991, Russia; <sup>b</sup>Department of Biochemistry, University of Turku, 20014 Turku, Finland; <sup>c</sup>Institute of Biotechnology, University of Helsinki, 00014 Helsinki, Finland; <sup>d</sup>Winogradsky Institute of Microbiology, Russian Academy of Sciences, Moscow 117312, Russia; <sup>e</sup>Department of Biotechnology, Delft University of Technology, 2628 BC Delft, The Netherlands; <sup>f</sup>Skryabin Institute of Biochemistry and Physiology of Microorganisms, Russian Academy of Sciences, Pushchino 142290, Russia; and <sup>g</sup>Microbial Systems Ecology, Department of Aquatic Microbiology, Institute for Biodiversity and Ecosystem Dynamics, University of Amsterdam, 1098 XH Amsterdam, The Netherlands

Edited by Harry B. Gray, California Institute of Technology, Pasadena, CA, and approved May 15, 2015 (received for review September 4, 2014)

**Cytochrome c oxidases (Coxs) are the basic energy transducers in the respiratory chain of the majority of aerobic organisms. Coxs studied to date are redox-driven proton-pumping enzymes belonging to one of three subfamilies: A-, B-, and C-type oxidases. The C-type oxidases (*cbb*<sub>3</sub> cytochromes), which are widespread among pathogenic bacteria, are the least understood. In particular, the proton-pumping machinery of these Coxs has not yet been elucidated despite the availability of X-ray structure information. Here, we report the discovery of the first (to our knowledge) sodium-pumping Cox (Scox), a *cbb*<sub>3</sub> cytochrome from the extremely alkaliphilic bacterium *Thioalkalivibrio versutus*. This finding offers clues to the previously unknown structure of the ion-pumping channel in the C-type Coxs and provides insight into the functional properties of this enzyme.**

cytochrome c oxidase | sodium pumping | *cbb*<sub>3</sub>-type oxidase | alkaliphily

The known terminal oxidases according to the structure of their active centers and their phylogenetic relations are subdivided into two superfamilies (1). One is composed of numerous representatives containing a heme-copper binuclear active center (BNC). Oxidases belonging to the other superfamily have no copper. This superfamily includes bacterial oxidases of the *bd* type. The superfamily of representatives with heme-copper BNC is subdivided in turn into two groups, cytochrome c oxidases (Coxs) and quinol oxidases, depending upon the electron donor, which can be either cytochrome *c* or quinol. Quinol oxidases with a heme-copper BNC are found only in prokaryotes, whereas Coxs are widespread among living organisms of all domains: Eukarya (where they are found in mitochondria and chloroplasts), Bacteria, and Archaea. Although terminal oxidases with heme-copper BNC constitute a diverse group of multisubunit enzymes having from 2 to 13 subunits, conservatism and similar architecture are obviously inherent in their main (catalytic) subunit. The catalytic center of the main subunit always contains two hemes and copper as redox active prosthetic groups and a redox active tyrosine covalently bound to histidine in the polypeptide chain (2–5). Iron of one of the hemes and copper constitute the BNC. Coxs are the best-studied group of terminal oxidases. The basic mechanism of energy transduction by Coxs during respiration consists of the oxidation of cytochrome *c* by molecular oxygen (O<sub>2</sub>) coupled to transmembrane pumping of protons (H<sup>+</sup>). This process results in reduction of O<sub>2</sub> to water by the BNC, where O<sub>2</sub> is bound. In Coxs, it requires four protons (“chemical” H<sup>+</sup> for water production) taken from the inner side of the membrane and can be coupled to the translocation of another four protons (“pumped” H<sup>+</sup>) from the inner to the outer side of the membrane into the intermembrane or the periplasmic space of mitochondria or prokaryotic cells, respectively, according to the following equation (6–8):



In A-type Coxs, two H<sup>+</sup> pathways in the main subunit were identified, the so-called D channel, conducting all pumped and part of chemical H<sup>+</sup>, and the K channel, conducting most of chemical H<sup>+</sup> (9). In C-type Coxs, only a K-channel analog was found (10). The described catalytic events are accomplished through generation of a transmembrane difference in H<sup>+</sup> potentials ( $\Delta\bar{\mu}_{\text{H}^{+}}$ ), which is used as a convertible membrane-linked biological currency. Microorganisms living in an alkaline environment maintain a nearly neutral cytoplasmic pH (11). This presents a problem for alkaliphiles because it gives rise to an inverted pH gradient that decreases the  $\Delta\bar{\mu}_{\text{H}^{+}}$  (12, 13). Some alkaliphilic microorganisms solve this problem by using an Na<sup>+</sup>-pumping NADH-CoQ reductase (NQR) (14), and perhaps a Na<sup>+</sup>-pumping terminal oxidase, as was assumed (15). At present, NQR is the only respiratory chain enzyme for which Na<sup>+</sup> pumping has been directly and undoubtedly established (16). However, NQR is absent in the extremely alkaliphilic bacterium *Thioalkalivibrio versutus* AL2, which inhabits an alkaline (~pH 10) Siberian soda lake at saturating salt

## Significance

The majority of aerobic living organisms use oxygen for respiration. The key enzyme, which directly reduces oxygen to water during respiration, is the terminal cytochrome c oxidase. It generates a large portion of the utilizable energy provided by the respiratory chain. Accumulation of biologically available energy by means of cytochrome c oxidases is believed to be due to the proton-motive force across the mitochondrial or bacterial membrane. Details of this energy conversion are still unclear. Here we report the discovery of a sodium-pumping cytochrome c oxidase that converts energy of respiration into sodium-motive force. This finding provides clues to understanding the mechanism of cytochrome c oxidase that is not available when applying knowledge of the proton-pumping versions of the enzyme.

Author contributions: M.S.M., D.A.B., R.L., and V.P.S. designed research; M.S.M., A.M.M., D.A.B., D.Y.S., I.I.S., T.V.I., and G.M. performed research; M.S.M. computed molecular modeling; D.A.C. performed molecular dynamic computation and molecular modeling; M.S.M., D.A.C., A.M.M., D.A.B., D.Y.S., I.I.S., T.V.I., R.L., G.M., and V.P.S. analyzed data; and M.S.M., D.A.C., D.A.B., and V.P.S. wrote the paper.

The authors declare no conflict of interest.

This article is a PNAS Direct Submission.

Data deposition: The nucleotide sequences of *Thioalkalivibrio cbb*<sub>3</sub> oxidase have been deposited in the EMBL database (accession no. HE575403.1).

<sup>1</sup>To whom correspondence may be addressed. Email: muntyan@genebee.msu.ru or skulach@genebee.msu.ru.

<sup>2</sup>Deceased March 13, 2014.

<sup>3</sup>Deceased November 9, 2012.

This article contains supporting information online at [www.pnas.org/lookup/suppl/doi:10.1073/pnas.1417071112/-DCSupplemental](http://www.pnas.org/lookup/suppl/doi:10.1073/pnas.1417071112/-DCSupplemental).

concentrations (17). *T. versutus* is a chemolithotroph that oxidizes sulfur compounds and employs Cox as a terminal component of its aerobic electron transport chain. Here we report that *T. versutus* uses a novel C-type Cox that (i) specifically requires  $\text{Na}^+$  for its activity and (ii) electrogenically exports  $\text{Na}^+$  from cells or right-side-out subcellular membrane vesicles, the process being coupled to oxidation of ascorbate by  $\text{O}_2$ .

## Results and Discussion

Experiments were performed using *T. versutus* cells (exhausted of endogenous substrates) and the right-side-out subcellular vesicles derived from them. Thus, both cells and vesicles displayed no respiration without substrate addition. To start respiration at the level of Coxs in respiratory chain, we used the exogenous substrates Wurster's blue [*N,N,N',N'*-tetramethyl-*p*-phenylenediamine (TMPD)], which is nonspecific for all terminal oxidases, or cytochrome *c*, which is specific for Coxs, both in the presence of a reductant ascorbate. Addition of any of the substrates initiated rapid  $\text{O}_2$  consumption (Fig. 1 *A* and *B*) and generation of an electric membrane potential ( $\Delta\psi$ ) (Fig. 1*D*). Similar to the  $\text{Na}^+$ -motive NQR (14), these activities were specifically  $\text{Na}^+$ -dependent, showing optimum at alkaline pH (8.5–9.5) (Fig. 1 *C* and *D*). In contrast, the well-known  $\text{H}^+$ -motive Coxs from *Rhodobacter sphaeroides* (7) and *Paracoccus denitrificans*, used as controls (Fig. S1 *A–C*), as well as from *Pseudomonas stutzeri* (18), showed no  $\text{Na}^+$  specificity (SI Text, section S1). Cytochrome *c*, unlike TMPD, was inefficient toward *T. versutus* Cox at high salt concentrations, similar to Coxs from other species; therefore, TMPD was used later on. The Cox inhibitor cyanide fully arrested both Cox activities (Fig. 1*D* and Fig. S1*D*). Thus, Cox operating in *T. versutus* membranes is a  $\text{Na}^+$ -dependent oxidase (Scox) that can be either a  $\text{Na}^+$ -activated  $\text{H}^+$  pump or  $\text{Na}^+$ -activated redox loop lacking in  $\text{H}^+$  pump.

To discriminate between these two possibilities, we tested  $\text{H}^+$  pumping by the oxidase. Unlike  $\text{H}^+$ -pumping Coxs, which acidify the external medium during respiration in the presence of the  $\text{K}^+$  ionophore valinomycin (Fig. S2*A*) (see also refs. 7 and 19), Scox

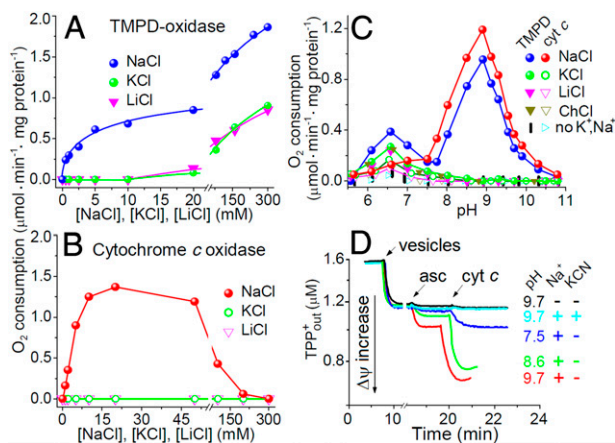


**Fig. 1.**  $\text{Na}^+$  concentration and pH dependence of the respiration-linked characteristics of cytochrome oxidase in *T. versutus* membrane vesicles. (*A–C*)  $\text{O}_2$  consumption and (*D*)  $\Delta\psi$  generation measured using tetraphenylphosphonium ( $\text{TPP}^+$ )-selective electrode; reactions were induced by substrate addition. Reaction media: 50 mM CHES-Tris buffer (pH 9.2) and 0.5 mM EDTA (*A* and *B*) or 50 mM Mops/TAPS/CAPS buffer-KOH, 0.5 mM EDTA, and 20 mM Na, K, Li, or choline (Ch) chloride (*C*) or 50 mM Mops/TAPS/CAPS buffer-KOH, 0.5 mM EDTA, and 30 mM  $\text{K}_2\text{SO}_4$  (no  $\text{Na}^+$ ) or 20 mM  $\text{Na}_2\text{SO}_4$ , 10 mM  $\text{K}_2\text{SO}_4$  (+ $\text{Na}^+$ ), 1.6  $\mu\text{M}$   $\text{TPP}^+$ , and 10  $\mu\text{M}$  KCN, where indicated (*D*). Vesicle protein concentration: 34  $\mu\text{g}/\text{mL}$  (*A–C*); 1  $\text{mg}/\text{mL}$  (*D*). Substrate final concentrations, 80  $\mu\text{M}$  TMPD (*A* and *C*) or 6  $\mu\text{M}$  horse heart cytochrome *c* (*B–D*), both in the presence of reductant, 2 mM ascorbate-Tris (pH 7) (*A–D*).

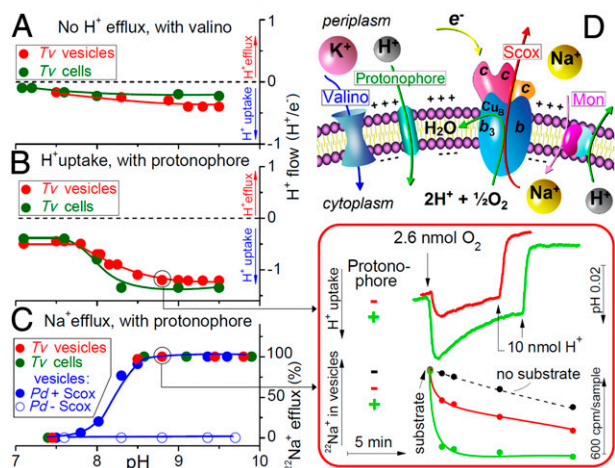


**Fig. 2.** pH profile of respiration-driven  $^{22}\text{Na}^+$  efflux and  $\text{H}^+$  uptake mediated by *T. versutus* AL2 (*Tv*) Scox. (*A*) The absence of  $\text{O}_2$  pulse-induced  $\text{H}^+$  pumping in *Tv* cells and right-side-out vesicles (“vesicles”) in the presence of 1  $\mu\text{M}$  valinomycin (valino). (*B*)  $\text{O}_2$  pulse-induced  $\text{H}^+$  uptake in *Tv* cells and vesicles in the presence of protonophore: 50  $\mu\text{M}$  CCCP (cells) or 25  $\mu\text{M}$  HQNO (vesicles). (*C*) Protonophore-supported  $\text{Na}^+$  pumping in  $^{22}\text{Na}^+$ -loaded *Tv* cells and vesicles and in *P. denitrificans* vesicles (*Pd-Scox*) and vesicles from Scox-expressing *P. denitrificans* (*Pd+Scox*).  $^{22}\text{Na}^+$  efflux was assessed for 2 min after substrate addition.  $\text{Na}^+$  efflux at pH 9 is defined as 100% in each case. Reactions were started by addition of  $\text{O}_2$  as small aliquots of water into an anaerobic reaction mixture (*A* and *B*) or ascorbate and TMPD (*C*). (*Inset*) Time scale, respiration-driven  $^{22}\text{Na}^+$  efflux (bottom) and  $\text{H}^+$  uptake (top) in *Tv* vesicles. For conditions, see Fig. 3 and Fig. S2. (*D*) Orientation of Scox and ion fluxes in bacterial cell and right-side-out membrane vesicles derived therefrom. Scox subunits as defined (Fig. S5): N (navy), O (orange), and P (pink). Scox active site facing the periplasm accepts electrons ( $e^-$ ) from a substrate and then pumps  $\text{Na}^+$  outside the cell; protonophore or  $\text{K}^+$  ionophore valino facilitates  $\text{Na}^+$  efflux via counter ion influx ( $\text{H}^+$  or  $\text{K}^+$ , respectively); the  $\text{Na}^+/\text{H}^+$ -antiporter monensin (Mon) collapses the  $\text{Na}^+$  gradient.

did not mediate  $\text{H}^+$  extrusion at alkaline pH (Fig. 2*A* and Fig. S2*B*), as shown earlier (20). Instead, Scox evoked alkalization of the medium in response to  $\text{O}_2$  pulse when valinomycin was replaced by protonophore, and  $\text{H}^+$  could serve as counter ion instead of  $\text{K}^+$  (Fig. 2*B* and inset and Fig. S2*C*). Reversibility of this alkalization in the time scale (upper green curve, Fig. 2, *Inset*) points that it cannot be attributed to  $\text{H}^+$  consumption during respiratory chemical reaction of water production because of irreversibility of the latter reaction. These effects could be explained by assuming that the oxidase is  $\text{Na}^+$ -motive and electrogenic. In such case,  $\Delta\psi$  formed by  $\text{Na}^+$  efflux, in the presence of a protonophore, should be counterbalanced by  $\text{H}^+$  influx, leading to reversible alkalization of the outer space. Fig. 2*D* shows these relationships. Consistent with this scheme, a respiration-driven, fully cyanide-sensitive export of  $^{22}\text{Na}^+$  was found in bacterial cells and vesicles preloaded with this isotope (Figs. 2*C* and 3*A* and *B*). Export of  $^{22}\text{Na}^+$  could be stimulated by protonophores [carbonyl cyanide *m*-chlorophenylhydrazone (CCCP) and 2-heptyl-4-hydroxyquinoline *N*-oxide (HQNO), a protonophore operating at alkaline pH (Fig. S3 and SI Text, section S2)] as well as valinomycin. Like respiratory activity of *T. versutus* Scox, export of  $^{22}\text{Na}^+$  occurred at alkaline pH (8.0–10.0) (Fig. 2*C*). These data confirm that *T. versutus* Scox operates as a primary  $\text{Na}^+$  pump rather than an  $\text{Na}^+/\text{H}^+$  antiporter or a  $\text{K}^+$  pump.

To identify the  $\text{Na}^+$ -pumping Scox, we considered the three known types of Coxs (21, 22): A, B, and C (Fig. 4*A*), which are represented by cytochromes *aa3/caa3*, *ba3*, and *cbb3*, respectively. Because *T. versutus* membranes contained heme B but not heme A (Fig. S4), A- and B-type Coxs can be excluded in our case. Instead, we identified an operon of a *cbb3* oxidase (C-type Cox)

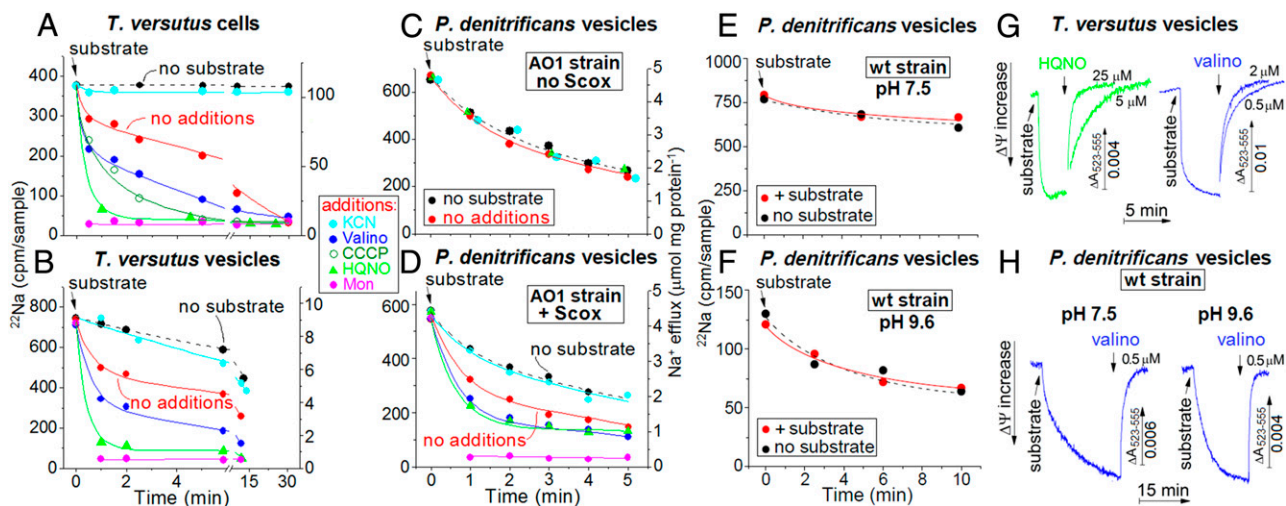


**Fig. 3.** Evidence of a primary  $\text{Na}^+$  pump in *T. versutus* (*Tv*). (A) Substrate-induced  $\text{Na}^+$  efflux from  $^{22}\text{Na}$ -loaded *Tv* cells, (B) *Tv* vesicles, (C) *P. denitrificans* AO1 vesicles without *Tv cbb*<sub>3</sub> (no *Scox*), (D) *P. denitrificans* AO1 vesicles with *Tv cbb*<sub>3</sub> (+*Scox*), and (E and F) WT *P. denitrificans* vesicles was assessed by radioactivity of  $^{22}\text{Na}$  retained in cells or vesicles after substrate addition. (G) Substrate-induced  $\Delta\psi$  generation in vesicles from *Tv* and (H) WT *P. denitrificans* monitored by spectral changes of safranin O (10  $\mu\text{M}$ ). A pH 9.2 (A–D and G), 7.5 (E and H), and 9.6 (F and H) reaction medium for “ $\text{Na}^+$  transport measurements” was used (Materials and Methods). Additions (final concentrations): valinomycin, 0.5  $\mu\text{M}$  (B, D, G, and H) or 2  $\mu\text{M}$  (A and G); protonophores: HQNO, 5  $\mu\text{M}$  (G), 25  $\mu\text{M}$  (B–D and G) or 50  $\mu\text{M}$  (A), and CCCP, 38  $\mu\text{M}$  (A); monensin, 0.1  $\mu\text{M}$  (B and D) or 38  $\mu\text{M}$  (A); KCN, 1 mM (B–D) or 10 mM (A); protein of cells, 2.7 mg/mL (A), vesicles, 0.7 mg/mL (B), 1 mg/mL (C–F), 50  $\mu\text{g/mL}$  (Left) or 76  $\mu\text{g/mL}$  (Right) (G), and 50 mg/mL (H). Arrows at “0” time show substrate addition: TMPD, 40  $\mu\text{M}$  (A, B, G, and H), or 3 mM (C–F) in the presence of ascorbate, 3 mM (B, G, and H) or 10 mM (A and C–F).

in the *T. versutus* genome (EMBL accession no. HE575403.1) and detected its expression product (Fig. S5 and SI Text, section S1; for the enzyme pattern, see Fig. 2D), which might operate in

this bacterium as a  $\text{Na}^+$  pump. Consistent with our hypothesis, *P. denitrificans* AO1 vesicles, which lack all Coxs and displayed no active  $\text{Na}^+$  transport (Figs. 2C and 3C), became capable of

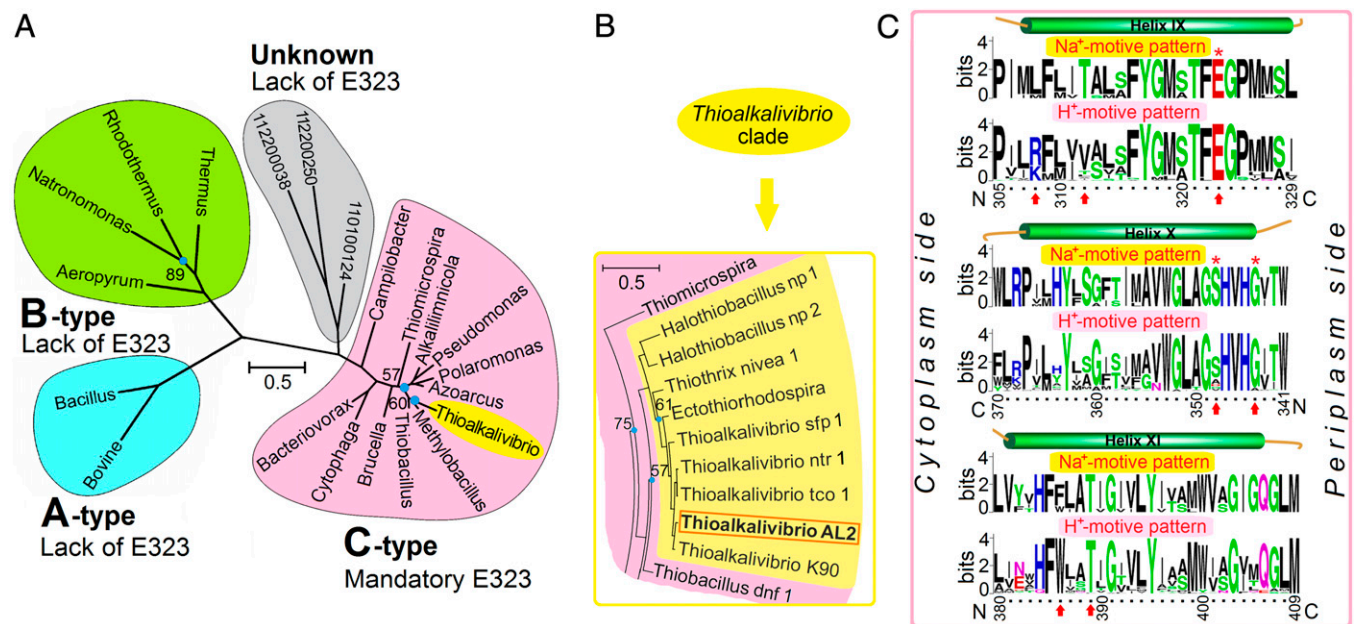


**Fig. 4.** Phylogenetic relationships of representative Coxs based on catalytic subunit protein sequences (Table S1). (A) The brief phylogenetic tree with representative Coxs: A-type (blue), B-type (green), and C-type (pink). *Thioalkalivibrio* clade (yellow, see also B) with R(K)308L(M) substitution is inside C-type Coxs. The sequences given in ref. 10 (gray) cluster separately from C-type Coxs (Unknown). E323 is conserved only in the catalytic subunit of C-type Coxs (see C); residue numbering corresponds to *P. stutzeri cbb*<sub>3</sub> (here and elsewhere). (B) Inset derived from the detailed phylogenetic tree with representative Coxs (Fig. S6); *T. versutus cbb*<sub>3</sub> *Scox* is orange-contoured. Blue spheres indicate nodes with clade credibility values <90; other nodes have clade credibility values  $\geq 90$ . (Scale bar: 0.5 substitutions per residue.) (C) Amino acid sequences of helices IX–XI of catalytic subunit of C-type Coxs aligned using WebLogo software (23). The upper panels of each pair under an individual  $\alpha$ -helix contain representatives of the  $\text{Na}^+$ -motive-like *cbb*<sub>3</sub> Coxs (yellow-colored in the C-type cluster); the lower panels contain all other representatives of the C-type cluster that are  $\text{H}^+$ -motive-like (pink-colored in the C-type cluster). Red arrows show R(K)308L(M) substitution and conservative T312, G344, S348, and T389 in the  $\text{Na}^+$ -motive-like representatives, E323 conserved in both groups, W386 conserved among  $\text{H}^+$ -motive-like representatives. Red asterisks in the  $\text{Na}^+$ -motive template indicate residues forming  $\text{Na}^+$  coordination shell (shown in Fig. 5B).

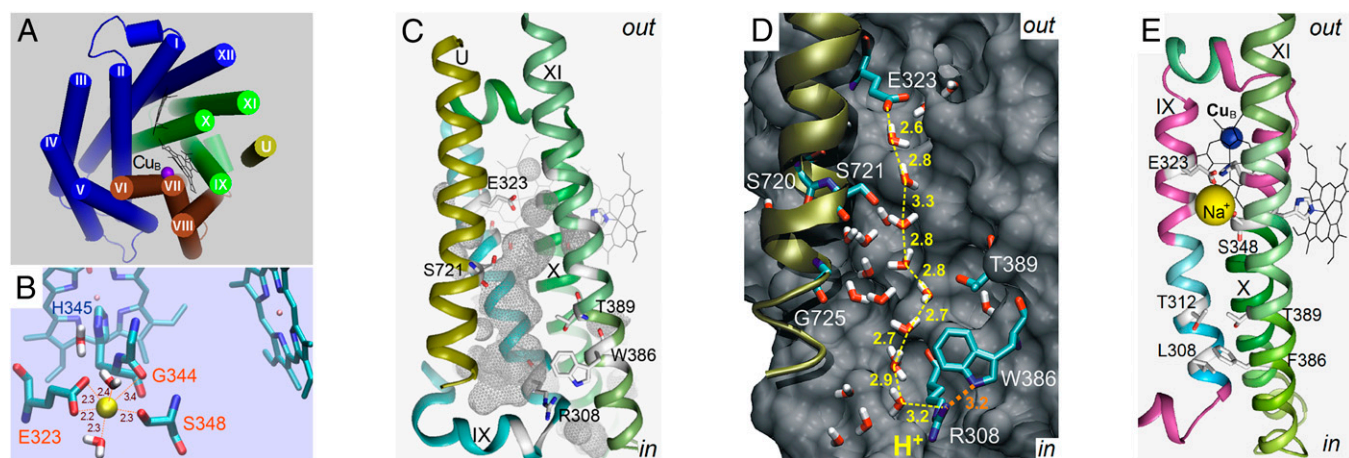


**Fig. 5.** Structural model of the ion-pumping channel in *cbb<sub>3</sub>* oxidases. (A) Cylindrical helix model of *P. stutzeri cbb<sub>3</sub>* catalytic subunit (ccoN) and  $\alpha$ -helix U (olive), viewed from periplasm (PDB ID code 3MK7). Helices VI–VIII (brown) form a “K channel” that conducts  $H^+$  for water production in the active center of all *cbb<sub>3</sub>* Coxs; helices IX–XI (green) form the proposed  $Na^+$ -pumping channel in  $Na^+$ -motive *cbb<sub>3</sub>* Coxs. (B)  $Na^+$  (yellow ball)-binding coordination shell in the active center in ccoN of *T. versutus cbb<sub>3</sub>*. It involves Glu323, Gly344, Ser348, and two water molecules as evaluated by VMD (27). (C) Large cavity (gray network) within  $\alpha$ -helices IX–XI (green and cyan) and U (olive) of *P. stutzeri cbb<sub>3</sub>*. Helix U, unresolved in the X-ray structure (26), was assigned to the ccoH sequence of *P. stutzeri cbb<sub>3</sub>* (SI Text, section S3 and ref. 28) (see also D). (D) Transient  $H^+$ -conducting network predicted at the interface between ccoN and the  $\alpha$ -helix U (olive) of  $H^+$ -motive *P. stutzeri cbb<sub>3</sub>*. (E) Assumed  $Na^+$ -translocating pathway in *T. versutus cbb<sub>3</sub>*; yellow ball marks hydrated  $Na^+$  ion. Regions in  $\alpha$ -helices lacking regularity (magenta) were predicted using DisEMBL Predictor (29). Images were made using PyMol (30) (A, C, and E) and VMD (27) (B and D).

oxidase-driven primary  $^{22}Na^+$  pumping (Figs. 2C and 3D) similar to that of *T. versutus* vesicles (Figs. 2C and 3B) after expression of *T. versutus cbb<sub>3</sub>*. We checked whether the observed  $^{22}Na^+$  export from the energized cells and vesicles could be explained by a  $\Delta\psi$ -potentiated  $^{22}Na^+/Na^+$  exchange or specified by a potential-dependent  $Na^+$  channel. Because dissipation of  $\Delta\psi$  by valinomycin, as well as by protonophore (Fig. 3G), increased  $^{22}Na^+$  export in *T. versutus* vesicles (Fig. 3B), a passive  $\Delta\psi$ -potentiated  $^{22}Na^+/Na^+$  leakage or  $^{22}Na^+$  transfer through a  $\Delta\psi$ -activated  $Na^+$  channel can be excluded. Consistent with this conclusion is the absence of  $\Delta\psi$ -driven  $^{22}Na^+$  export in  $^{22}Na^+$ -loaded WT *P. denitrificans* vesicles that lack *T. versutus* Scox (Fig. 3E, F, and H). The data also reveal that *P. denitrificans aa<sub>3</sub>* and *cbb<sub>3</sub>* Coxs, expressed in the used growth conditions (Materials and Methods), do not pump  $Na^+$ . Thus, these experiments directly demonstrated that *T. versutus cbb<sub>3</sub>* is a primary  $Na^+$  pump.

The *cbb<sub>3</sub>* oxidases studied previously were shown to operate as  $H^+$  pumps (7, 19, 24, 25). However, an individual pathway of pumped  $H^+$  analogous to the D channel in A-type Coxs has not been identified (10, 24). Only a K-pathway analog, involved in delivering chemical  $H^+$  to BNC to produce water in Coxs of all types, has been experimentally and structurally (10, 25, 26, 31) defined in C-type Coxs (depicted by brown-colored helices in Fig. 5A). Based on these data (10, 33), the K-channel analog in C-type Coxs was proposed to also fulfill the role of the D channel. To localize a possible  $Na^+$ -pumping pathway in Scox, we compared  $Na^+$ - and  $H^+$ -motive structural models. Before comparing the two models, we performed phylogenetic analyses of the C-type Cox protein sequences. Evidently, *T. versutus* Scox clusters with eight other sequences from extremely haloalkaliphilic species deep in the type-C phylogeny, and thus it constitutes the *Thioalkalivibrio* clade (yellow-colored, Fig. 4A and B). Taking into consideration such clustering, we divided all protein sequences of the C-type Cox main subunit into two groups for further comparison: yellow-colored *Thioalkalivibrio* clade (including *T. versutus* AL2) and other, pink-colored clades (Fig. 4C and Fig. S7). The sequences were compared in view of 3D structure of C-type Cox. Because the catalytic subunit (ccoN) of the two *cbb<sub>3</sub>* Coxs— $Na^+$ -motive from *T. versutus* and  $H^+$ -motive from *P. stutzeri*—are highly similar (69% identity), we modeled the 3D structure of the *T. versutus* subunit based on *P. stutzeri* X-ray data

(26). We analyzed in detail the membrane-spanning parts of the model to identify the substitutions that govern ion specificity. Because the “K channel” formed by helices VI–VIII (Fig. 5A) does not contain specific substitutions across the *cbb<sub>3</sub>* cluster (Fig. S7), the “K channel” is not likely to mediate  $Na^+$  pumping. Instead, we found indications of the tentative  $Na^+$ -pumping channel located within helices IX–XI in the catalytic subunit of *T. versutus* and of homologs that occupy the same clade: (i) a unique substitution, R(K)308L(M), near the cytoplasmic entrance of the tentative  $Na^+$  channel and (ii) conservatism of residues T312, G344, S348, and T389 (Fig. 4C). Accordingly, we propose that within C-type Coxs these five residues serve as a fingerprint that distinguishes two templates of catalytic subunits:  $Na^+$ -motive-like (*Thioalkalivibrio* clade) and  $H^+$ -motive-like (all other C-type members). Additionally, W386 seemed to be fully conserved among the  $H^+$ -motive-like but not in the  $Na^+$ -motive-like C-type members.

Another indication that the  $Na^+$ -pumping channel is located within helices IX–XI in the *T. versutus* Scox is provided by the observation that there is a unique conserved, ionizable, membrane-embedded residue, E323, that is found in the middle of helix IX (Fig. 4C). This E323 is surrounded by several polar residues that form a  $Na^+$ -coordination shell and could function as  $Na^+$  chelators (Fig. 5B). In the *R. sphaeroides*  $H^+$ -motive *cbb<sub>3</sub>*, the corresponding glutamate (E383) was initially suggested to participate in  $H^+$  pumping (24). However, its functional role in  $H^+$  pumping was challenged later based on the absence of E323 in some putative C-type Coxs (10). To resolve discrepancies about the role of E323, we performed phylogenetic analyses of the C-type Cox sequences used in ref. 10 where the study was limited to sequence-alignment level. We found that the previously assigned C-type Cox sequences that lack E323 do not actually cluster with other C-type enzymes in the phylogenetic tree and form a phylogenetically distinct clade (gray-colored, Fig. 4A and Fig. S6), which we tentatively define as a group with unknown function. In our designation, the C-type Cox family covers the sequences from *Campylobacter* to *Bacteriovorax* in the phylogenetic tree (pink and yellow clusters, Fig. 4A and B and Fig. S6). Significantly, E323 is fully conserved in these C-type sequences, but it is never present in other Cox types.

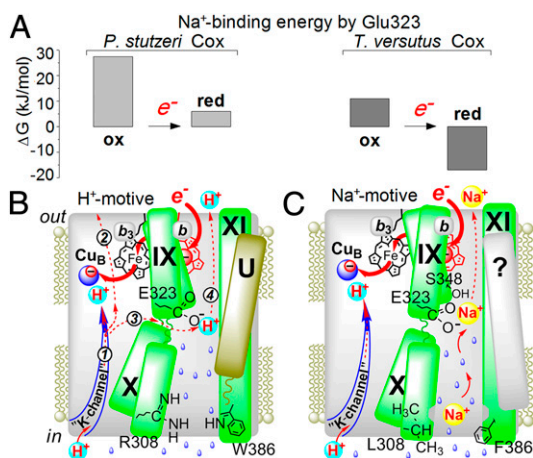
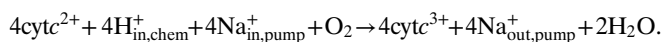


**Fig. 6.** Putative mechanism of ion translocation by the H<sup>+</sup>-motive (*P. stutzeri*) and Na<sup>+</sup>-motive (*T. versutus*) *cbb*<sub>3</sub> Coxs for a single electron transfer. (A) Free energy of Na<sup>+</sup> binding by E323 in *ccoN* of *P. stutzeri* (left) and *T. versutus cbb*<sub>3</sub> (right), estimated by the free energy perturbation method within MD modeling of the complexes in 1 M Na<sup>+</sup> solution (Table S2). (B) Combined models of the H<sup>+</sup>-pumping channel in the H<sup>+</sup>-motive *cbb*<sub>3</sub> by several hypotheses (circled numbers): 1 (10) + 2 (26) or 1 + 3 (26, 32) + 4 (24). (C) Functional model of the sodium pumping in the Na<sup>+</sup>-motive *cbb*<sub>3</sub> (this study) formed by  $\alpha$ -helices IX–XI (green) of the catalytic subunit;  $\alpha$ -helix (question-marked rectangle) in the Na<sup>+</sup>-motive Cox analogous to the auxiliary  $\alpha$ -helix U (olive) in the H<sup>+</sup>-motive Cox is presumed. In the H<sup>+</sup>-motive and Na<sup>+</sup>-motive *cbb*<sub>3</sub> Coxs, a large gray rectangle depicts helices I–VIII and XII: “K channel” (blue) delivers chemical H<sup>+</sup> to the active center to produce water during reduction of O<sub>2</sub>.

Notably, helices IX and X of the catalytic subunit of *P. stutzeri cbb*<sub>3</sub> (H<sup>+</sup>-motive pattern) as well as of *T. versutus cbb*<sub>3</sub> (Na<sup>+</sup>-motive pattern) contain features that disrupt regularity of the helices, conferring flexibility that might be necessary for ion transfer (Fig. 5E). Additionally, in *P. stutzeri cbb*<sub>3</sub> the only large cavity seems to be located within helices IX–XI of the main subunit (Fig. 5C) and the recently identified auxiliary subunit U (26) (for details, see SI Text, section S3). When water-filled, this cavity could link the critical residues R(K)308 and E323, providing a water-filled H<sup>+</sup>-translocation pathway (Fig. 5D). These facts allow us to assume that in the Na<sup>+</sup>-motive *cbb*<sub>3</sub> such cavity could serve as the Na<sup>+</sup>-pumping channel. Finally, we evaluated the Na<sup>+</sup>-binding capacity of the H<sup>+</sup>-motive and Na<sup>+</sup>-motive *cbb*<sub>3</sub> Coxs using molecular dynamics (MD). MD simulations predicted that the main subunit of *T. versutus*, but not that of *P. stutzeri*, can bind Na<sup>+</sup> in the E323 site in a redox-linked manner (Fig. 6A and B and Table S2). According to the prediction, one electron coming into the metal active center switches the enzyme from a Na<sup>+</sup>-nonbinding oxidized (ox) state to a Na<sup>+</sup>-binding reduced (red) state. Under the tentative model, the subsequent entry of H<sup>+</sup> to the active center via the chemical reaction through the “K channel” results in Na<sup>+</sup> extrusion (Fig. 6B). The predicted coupling stoichiometry is one electron for each pumped Na<sup>+</sup>, which is consistent with the experimental data (Fig. 2B and Fig. S2 B and C) according to which *S*<sub>cox</sub> operation fits in best with the following equation:



Evidently, the capacity of *T. versutus S*<sub>cox</sub> to bind Na<sup>+</sup> is provided by the E323-involving Na<sup>+</sup>-coordination shell (see Fig. 5B), which is absent in *P. stutzeri* Cox due to S348(A) substitution.

The fact that the Na<sup>+</sup>-pumping function was revealed among C-type Coxs may shed light on evolution of Coxs. At present, the phylogenomics-based evolutionary scenario of Coxs remains

obscure (1, 22, 34). Therefore, in our reasoning we take into consideration several independent markers of possible Cox evolution and generally accepted facts: (i) geological evidence on oxygen-free atmosphere on the Earth preceded an oxygen atmosphere (35), (ii) close relationship between nitric oxide reductases and C-type Coxs and their far distance from A- and B-type Coxs (1, 36, 37), and (iii) the conclusion that Na<sup>+</sup> energetics appeared before H<sup>+</sup> energetics (38). If we believe the mentioned facts and views are true, then C-type Coxs—which include Na<sup>+</sup>-motive and H<sup>+</sup>-motive representatives—might be the ancestors of H<sup>+</sup>-motive A- and B-type Coxs, as assumed earlier (37). C-type Coxs were shown to bind O<sub>2</sub> much more tightly than A-type Coxs (39). Owing to this property C-type Coxs operate under low O<sub>2</sub> conditions and would be the first energy-transducing enzymes capable of oxygen reduction when the early atmosphere of the Earth was formed, being gradually filled with O<sub>2</sub>.

## Conclusion

We provide the first direct demonstration to our knowledge that the *T. versutus* cytochrome *cbb*<sub>3</sub> (Cox) is a primary Na<sup>+</sup> pump. This finding is collectively based on the observation of (i) specific Na<sup>+</sup> dependence of Cox activity, (ii) protonophore- or valinomycin-stimulated Na<sup>+</sup> pumping in *T. versutus* cells and vesicles, (iii) no H<sup>+</sup> pumping in them in the presence of valinomycin and reversible alkalization of the outer space in the presence of protonophore without valinomycin, (iv) expression of the *T. versutus cbb*<sub>3</sub> in *P. denitrificans* cells with the result that membranes of this bacterium are competent in protonophore/valinomycin-activated respiration-supported Na<sup>+</sup> pumping, and (v) a Na<sup>+</sup>-binding coordination shell in the active center of Cox. These results raise the question of whether Na<sup>+</sup> pumping is inherent in some other C-type Coxs. In this context, whether the Na<sup>+</sup> transport in *Vitreoscilla* (40) is evoked by a primary Na<sup>+</sup>-pumping *bo*-type quinol oxidase or by a secondary pumping Na<sup>+</sup>/H<sup>+</sup> antiporter is still unclear for the lack of ionophore tests after *bo* oxidase expression in *Escherichia coli*, which contains self-Na<sup>+</sup>/H<sup>+</sup> antiporters (41) (for details, see SI Text, section S2). Our findings are consistent with the hypothesis of using Na<sup>+</sup>-motive energy transducers in organisms living under low  $\Delta$ pH and high salinity (12) and might stimulate further progress in the study of energy-transduction mechanisms of Coxs.

## Materials and Methods

Cultivation of bacterial strains, phylogenetic analysis, molecular dynamic simulations, and other methods are detailed in SI Materials and Methods.

**Bacterial Strains.** *T. versutus* AL2 and *P. denitrificans* strain AO1 [expresses no cytochrome c oxidase activity (42)] and WT strain (PD 1222) were batch-cultured aerobically as previously described (17, 43).

**Membrane Vesicle Isolation.** Right-side-out membrane vesicles were isolated from freshly grown cells in a medium containing 50 mM CAPSO-KOH (pH 9.9), 50 mM K<sub>2</sub>SO<sub>4</sub>, 0.1 M sucrose, 0.1 mM EGTA, and 0.35 M Na<sub>2</sub>SO<sub>4</sub> by disruption in a French press cell according to a standard procedure.

**Expression of Coxs in *P. denitrificans*.** For heterologous expression of *T. versutus cbb*<sub>3</sub> Cox in *P. denitrificans*, the *T. versutus* AL2 *ccoNOQP* operon was identified (HE575403.1) and amplified by PCR. The PCR fragment was cloned into the XbaI-HindIII-digested derivative of the broad host-range plasmid pBBR1MCS (42, 43) to produce the pBBR1/*ccoNOQP* plasmid. For protein expression, the recombinant plasmid pBBR1/*ccoNOQP* was transferred by conjugation into the *Paracoccus* recipient strain AO1. Exogenously expressed *T. versutus cbb*<sub>3</sub> Cox in strain AO1 reached a level comparable to that in *T. versutus* AL2 strain, as monitored using Western blotting. Expression of self-*cbb*<sub>3</sub> Cox in *P. denitrificans* WT strain grown aerobically (this study) reached the same high level as in semiaerobically grown cells (44), as quantified by real-time quantitative PCR. Each self-Cox level, *aa*<sub>3</sub> and *cbb*<sub>3</sub>, reached 70 pmol Cox/mg of membrane protein as determined by CO-reduced minus reduced spectra using extinction coefficients of 7 mM<sup>-1</sup>·cm<sup>-1</sup>

( $aa_3$ , 595–606 nm) (45) and  $7.6 \text{ mM}^{-1} \cdot \text{cm}^{-1}$  ( $cbb_3$ , 558–572 nm) (46). Self-Coxs presence was confirmed by the laser-flash photolysis method (47).

$\text{Na}^+$  transport measurements were performed with starved bacterial cells exhausted of endogenous substrates and loaded with  $^{22}\text{Na}^+$  (PerkinElmer Life Sciences) on ice as reported (48). Membrane vesicles were loaded with  $^{22}\text{Na}^+$  by passive diffusion (incubation medium: 50 mM CAPSO/TRICINE/Mops-KOH, 50 mM  $\text{K}_2\text{SO}_4$ , 0.1 M sucrose, 0.1 mM EGTA, and 0.6 M  $\text{Na}_2\text{SO}_4$ ) at 6 °C overnight. Then  $^{22}\text{Na}^+$ -loaded cells or vesicles were added to the “cold”- $\text{Na}^+$ -containing incubation medium and the reaction was started by addition of substrate together with ascorbate (at 22°C). Samples of 25  $\mu\text{L}$  were withdrawn from the incubation mixture at the appointed time and cells or vesicles were separated from the incubation medium by rapid vacuum filtration (1–3 s) through nitrocellulose filters (Millipore). Radioactivity was counted using a liquid scintillation counter (LKB Wallac 1215 RackBeta). Each curve shown in figures is the average of three to eight independent experiments.

- Gribaldo S, Talla E, Brochier-Armanet C (2009) Evolution of the haem copper oxidases superfamily: a rooting tale. *Trends Biochem Sci* 34(8):375–381.
- Rauhamaäki V, Bloch DA, Verkhovsky MI, Wikström M (2009) Active site of cytochrome  $cbb_3$ . *J Biol Chem* 284(17):11301–11308.
- Rauhamaäki V, Baumann M, Soliymani R, Puustinen A, Wikström M (2006) Identification of a histidine-tyrosine cross-link in the active site of the  $cbb_3$ -type cytochrome c oxidase from *Rhodobacter sphaeroides*. *Proc Natl Acad Sci USA* 103(44):16135–16140.
- Oztürk M, Watmough NJ (2011) Mutagenesis of tyrosine residues within helix VII in subunit I of the cytochrome  $cbb_3$  oxidase from *Rhodobacter capsulatus*. *Mol Biol Rep* 38(5):3319–3326.
- Kaila VRI, Johansson MP, Sundholm D, Laakkonen L, Wikström M (2009) The chemistry of the  $\text{Cu}_B$  site in cytochrome c oxidase and the importance of its unique His-Tyr bond. *Biochim Biophys Acta* 1787(4):221–233.
- Verkhovsky MI, Jasaitis A, Verkhovskaya ML, Morgan JE, Wikström M (1999) Proton translocation by cytochrome c oxidase. *Nature* 400(6743):480–483.
- Rauhamaäki V, Bloch DA, Wikström M (2012) Mechanistic stoichiometry of proton translocation by cytochrome  $cbb_3$ . *Proc Natl Acad Sci USA* 109(19):7286–7291.
- Rauhamaäki V, Wikström M (2014) The causes of reduced proton-pumping efficiency in type B and C respiratory heme-copper oxidases, and in some mutated variants of type A. *Biochim Biophys Acta* 1837(7):999–1003.
- Konstantinov AA, Siletsky S, Mitchell D, Kaulen A, Gennis RB (1997) The roles of the two proton input channels in cytochrome c oxidase from *Rhodobacter sphaeroides* probed by the effects of site-directed mutations on time-resolved electrogenic intraprotein proton transfer. *Proc Natl Acad Sci USA* 94(17):9085–9090.
- Hemp J, et al. (2007) Comparative genomics and site-directed mutagenesis support the existence of only one input channel for protons in the C-family ( $cbb_3$  oxidase) of heme-copper oxygen reductases. *Biochemistry* 46(35):9963–9972.
- Slonczewski JL, Fujisawa M, Dopson M, Krulwich TA (2009) Cytoplasmic pH measurement and homeostasis in bacteria and archaea. *Adv Microb Physiol* 55:1–79, 317.
- Skulachev VP (1984) Sodium bioenergetics. *Trends Biochem Sci* 9(11):483–485.
- Dimroth P, Cook GM (2004) Bacterial  $\text{Na}^+$  - or  $\text{H}^+$  -coupled ATP synthases operating at low electrochemical potential. *Adv Microb Physiol* 49:175–218.
- Unemoto T, Hayashi M (1993)  $\text{Na}^+$ -translocating NADH-quinone reductase of marine and halophilic bacteria. *J Bioenerg Biomembr* 25(4):385–391.
- Semeykina AL, Skulachev VP, Verkhovskaya ML, Bulygina ES, Chumakov KM (1989) The  $\text{Na}^+$ -motive terminal oxidase activity in an alkalo- and halo-tolerant *Bacillus*. *Eur J Biochem* 183(3):671–678.
- Häse CC, Fedorova ND, Galperin MY, Dibrov PA (2001) Sodium ion cycle in bacterial pathogens: Evidence from cross-genome comparisons. *Microbiol Mol Biol Rev* 65(3):353–370.
- Sorokin DY, et al. (2001) *Thioalkalimicrobium aerophilum* gen. nov., sp. nov. and *Thioalkalimicrobium sibiricum* sp. nov., and *Thioalkalivibrio versutus* gen. nov., sp. nov., *Thioalkalivibrio nitratris* sp. nov., novel and *Thioalkalivibrio denitrificans* sp. nov., novel obligately alkaliphilic and obligately chemolithoautotrophic sulfur-oxidizing bacteria from soda lakes. *Int J Syst Evol Microbiol* 51(Pt 2):565–580.
- Xie H, Buschmann S, Langer JD, Ludwig B, Michel H (2014) Biochemical and biophysical characterization of the two isoforms of  $cbb_3$ -type cytochrome c oxidase from *Pseudomonas stutzeri*. *J Bacteriol* 196(2):472–482.
- Han H, et al. (2011) Adaptation of aerobic respiration to low  $\text{O}_2$  environments. *Proc Natl Acad Sci USA* 108(34):14109–14114.
- Grishuk YV, Muntyan MS, Popova IV, Sorokin DY (2003) Ion transport coupled to terminal oxidase functioning in the extremely alkaliphilic halotolerant bacterium *Thioalkalivibrio*. *Biochemistry (Mosc)* 68(4):385–390.
- Pereira MM, Santana M, Teixeira M (2001) A novel scenario for the evolution of haem-copper oxygen reductases. *Biochim Biophys Acta* 1505(2–3):185–208.
- Sousa FL, et al. (2012) The superfamily of heme-copper oxygen reductases: Types and evolutionary considerations. *Biochim Biophys Acta* 1817(4):629–637.
- Crooks GE, Hon G, Chandonia JM, Brenner SE (2004) WebLogo: A sequence logo generator. *Genome Res* 14(6):1188–1190.
- Sharma V, Puustinen A, Wikström M, Laakkonen L (2006) Sequence analysis of the  $cbb_3$  oxidases and an atomic model for the *Rhodobacter sphaeroides* enzyme. *Biochemistry* 45(18):5754–5765.
- Lee HJ, Gennis RB, Ådelroth P (2011) Entrance of the proton pathway in  $cbb_3$ -type heme-copper oxidases. *Proc Natl Acad Sci USA* 108(43):17661–17666.
- Buschmann S, et al. (2010) The structure of  $cbb_3$  cytochrome oxidase provides insights into proton pumping. *Science* 329(5989):327–330.
- Humphrey W, Dalke A, Schulten K (1996) VMD: Visual molecular dynamics. *J Mol Graph* 14(1):33–38, 27–28.
- Ekici S, Pawlik G, Lohmeyer E, Koch H-G, Daldal F (2012) Biogenesis of  $cbb_3$ -type cytochrome c oxidase in *Rhodobacter capsulatus*. *Biochim Biophys Acta* 1817(6):898–910.
- Linding R, et al. (2003) Protein disorder prediction: Implications for structural proteomics. *Structure* 11(11):1453–1459.
- DeLano WL (2002) PyMOL Molecular Viewer. Available at www.pymol.org.
- Kaila VRI, Verkhovsky MI, Wikström M (2010) Proton-coupled electron transfer in cytochrome oxidase. *Chem Rev* 110(12):7062–7081.
- Sharma V, Wikström M, Kaila VRI (2012) Dynamic water networks in cytochrome  $cbb_3$  oxidase. *Biochim Biophys Acta* 1817(5):726–734.
- Ahn YO, et al. (2014) Conformational coupling between the active site and residues within the  $\text{K}^{\text{C}}$ -channel of the *Vibrio cholerae*  $cbb_3$ -type (C-family) oxygen reductase. *Proc Natl Acad Sci USA* 111(42):E4419–E4428.
- Docluzeau A-L, Ouchane S, Nitschke W (2008) The  $cbb_3$  oxidases are an ancient innovation of the domain bacteria. *Mol Biol Evol* 25(6):1158–1166.
- Schopf JW (2014) Geological evidence of oxygenic photosynthesis and the biotic response to the 2400–2200 Ma “Great oxidation event”. *Biochemistry (Mosc)* 79(3):165–177.
- Sousa FL, Alves RJ, Pereira-Leal JB, Teixeira M, Pereira MM (2011) A bioinformatics classifier and database for heme-copper oxygen reductases. *PLoS ONE* 6(4):e19117.
- Saraste M, Castresana J (1994) Cytochrome oxidase evolved by tinkering with denitrification enzymes. *FEBS Lett* 341(1):1–4.
- Mulkidjanian AY, Galperin MY, Makarova KS, Wolf YI, Koonin EV (2008) Evolutionary primacy of sodium bioenergetics. *Biol Direct* 3:13.
- Preisig O, Zufferey R, Thöny-Meyer L, Appleby CA, Hennecke H (1996) A high-affinity  $cbb_3$ -type cytochrome oxidase terminates the symbiosis-specific respiratory chain of *Bradyrhizobium japonicum*. *J Bacteriol* 178(6):1532–1538.
- Chung YT, Stark BC, Webster DA (2006) Role of Asp544 in subunit I for  $\text{Na}^+$  pumping by *Vitreoscilla* cytochrome *bo*. *Biochem Biophys Res Commun* 348(4):1209–1214.
- Krulwich TA, Sachs G, Padan E (2011) Molecular aspects of bacterial pH sensing and homeostasis. *Nat Rev Microbiol* 9(5):330–343.
- Pfützner U, et al. (1998) Cytochrome c oxidase (heme  $aa_3$ ) from *Paracoccus denitrificans*: Analysis of mutations in putative proton channels of subunit I. *J Bioenerg Biomembr* 30(1):89–97.
- Riistama S, Laakkonen L, Wikström M, Verkhovsky MI, Puustinen A (1999) The calcium binding site in cytochrome  $aa_3$  from *Paracoccus denitrificans*. *Biochemistry* 38(33):10670–10677.
- Otten MF, Stork DM, Reijnders WN, Westerhoff HV, Van Spanning RJ (2001) Regulation of expression of terminal oxidases in *Paracoccus denitrificans*. *Eur J Biochem* 268(8):2486–2497.
- Ludwig B, Schatz G (1980) A two-subunit cytochrome c oxidase (cytochrome  $aa_3$ ) from *Paracoccus denitrificans*. *Proc Natl Acad Sci USA* 77(1):196–200.
- García-Horsman JA, Berry E, Shapleigh JP, Alben JO, Gennis RB (1994) A novel cytochrome c oxidase from *Rhodobacter sphaeroides* that lacks CuA. *Biochemistry* 33(10):3113–3119.
- Muntyan MS, Dinarieva TY, Baev MV, Netrusov AI (2002) Effect of growth conditions on the synthesis of terminal oxidases in *Methylobacillus flagellatus* KT. *Arch Biochem Biophys* 398(1):118–124.
- Nakamura T, Tokuda H, Unemoto T (1982) Effects of pH and monovalent cations on the potassium ion exit from the marine bacterium, *Vibrio alginolyticus*, and the manipulation of cellular cation contents. *Biochim Biophys Acta* 692(3):389–396.
- Huttunen MT, Akerman KEO (1980) Measurements of membrane potentials in *Escherichia coli* K-12 inner membrane vesicles with the safranin method. *Biochim Biophys Acta* 597(2):274–284.
- Kamo N, Muratsugu M, Hongoh R, Kobatake Y (1979) Membrane potential of mitochondria measured with an electrode sensitive to tetraphenyl phosphonium and relationship between proton electrochemical potential and phosphorylation potential in steady state. *J Membr Biol* 49(2):105–121.
- Puustinen A, Finel M, Virkki M, Wikström M (1989) Cytochrome *o* (*bo*) is a proton pump in *Paracoccus denitrificans* and *Escherichia coli*. *FEBS Lett* 249(2):163–167.